Quantification of Multi-Parametric Magnetic Resonance Imaging Based on Radiomics Analysis for Differentiation of Benign and Malignant Lesions of Prostate

Soheila Koopaei (MSc)[1,2], Anahita Fathi Kazerooni (PhD)[2], Mahyar Ghafoori (MD)[3], Mohamadreza Alviri (MSc)[2], Fakhereh Pashaei (PhD)[1,4], Hamidreza Saligheh Rad (PhD)[1,2]*

[1]Quantitative MR Imaging and Spectroscopy Group, Research Center for Molecular and Cellular Imaging, Institute for Advanced Medical Technologies, Imam Hospital, Tehran, Iran
[2]Department of Medical Physics and Biomedical Engineering, School of Medicine, Tehran University of Medical Science Tehran, Iran
[3]Department of Radiology, Hazrat Rasoul Akram University Hospital, Tehran, Iran
[4]Radiation Sciences Research Center (RSRC), Aja University of Medical Sciences, Tehran, Iran

ABSTRACT

Background: The most common cancer (non-cutaneous) malignancy among men is prostate cancer. Management of prostate cancer, including staging and treatment, playing an important role in decreasing mortality rates. Among all current diagnostic tools, multiparametric MRI (mp-MRI) has shown high potential in localizing and staging prostate cancer. Quantification of mp-MRI helps to decrease the dependency of diagnosis on readers' opinions.

Objective: The aim of this research is to set a method based on quantification of mp-MRI images for discrimination between benign and malignant prostatic lesions with fusion-guided MR imaging/transrectal ultrasonography biopsy as a pathology validation reference.

Material and Methods: It is an analytical research that 27 patients underwent the mp-MRI examination, including T1- and T2- weighted and diffusion weighted imaging (DWI). Quantification was done by calculating radiomic features from mp-MRI images. Receiver-operating-characteristic curve was done for each feature to evaluate the discriminatory capacity and linear discriminant analysis (LDA) and leave-one-out cross-validation for feature filtering to estimate the sensitivity, specificity and accuracy of the benign and malignant lesion differentiation process is used.

Results: An accuracy, sensitivity and specificity of 92.6%, 95.2% and 83.3%, respectively, were achieved from a subset of radiomics features obtained from T2-weighted images and apparent diffusion coefficient (ADC) maps for distinguishing benign and malignant prostate lesions.

Conclusion: Quantification of mp-MRI (T2-weighted images and ADC-maps) based on radiomics feature has potential to distinguish benign with appropriate accuracy from malignant prostate lesions. This technique is helpful in preventing needless biopsies in patients and provides an assisted diagnosis for classifications of prostate lesions.

*Corresponding author:
Hamidreza Saligheh Rad
Department of Medical Physics and Biomedical Engineering, School of Medicine, Tehran University of Medical Science, Tehran, Iran
E-mail: h-salighehrad@tums.ac.ir

Introduction

The second most common cause of cancer-related deaths in men is prostate cancer [1]. Nowadays, the most important diagnostic tools for prostate cancer are based on: (1) screening the prostate-specific antigen (PSA), (2) digital rectal examination (DRE), and

(3) random systematic transrectal ultrasound-guided (TRUS) 12-core biopsy as the standard care [2].

PSA-based screening decreases the mortality rate by 21% [3]; however, its low diagnostic accuracy causes multiple issues. First, in 70%-80% of patients, the increase in PSA value is a sign of prostatitis and benign prostatic hyperplasia (BPH) and not the prostate cancer (PC). Moreover, in one-third of the population with normal PSA, the result of biopsy is positive for PC [4, 5].

DRE method is the primary test performed by a physician, and if the cancer tissue is localized, there is no chance of diagnosis using this method [6].

Although, TRUS-guided biopsy is the standard of care for PC, it is unable to differentiate prostate zonal anatomy for biopsy and has the false negative rate of 20% [7, 8]. Inaccurate tumor stratification of PCs causes underestimation of their aggressiveness [9] or overestimation of their stages [10] for over 30% of PCs. In addition, TRUS-guided biopsy can be associated with complications, especially urosepsis with large number of cases with antibiotic-resistant infection [11]. This infection rate also increases by the number of biopsy cores [12].

The existing low diagnostic accuracy in current tools might result in inaccurate staging. Therefore, management of prostate cancer is difficult due to fast rate of disease progression. Thus, despite their benefits, it is highly desirable to establish additional methods for increasing diagnostic accuracy and avoiding the unnecessary biopsies in patients with benign lesions.

Multiparametric magnetic resonance imaging (mp-MRI) provides anatomical and functional images of prostate gland [8]. It provides information about anatomy and tissue characteristics, such as volume and cellularity and is an accurate method to detect, localize, and stage prostate cancers [13]. In mp-MRI studies, high-resolution anatomical T2-weighted (T2w) imaging is combined with advanced imaging methods, such as diffusion-weighted imaging (DWI). One of its applications is to guide the biopsy procedure of the prostate. The systematic fused MRI-TRUS biopsy has higher sensitivity than TRUS, thus, the samples are taken from all different zones of the prostate and especially from suspicious areas in mp-MRI images. Nonetheless, fused MRI-TRUS biopsy is still invasive and creates issues such as infection, bleeding, and pain, similar to TRUS biopsy. Mp-MRI is especially valuable for avoiding biopsies in patients with clinical symptoms and decision making about the most appropriate treatment strategy for the patient [14].

Radiologists' qualitative research based on PIRADS (Prostate imaging report and data system) (v2) shows overlap between benign and malignant lesions in some cases. The signal decrease in T2w images of prostatic lesions is interpreted as the loss of water content in cancerous tissues [15]. However, prostatitis, hemorrhage, atrophy and benign prostatic hyperplasia (BPH) can also show low signal on T2w images, and may be mistaken for cancer.

Hypercellularity (as a property of cancer) and destruction of normal glandular tissue cause the diffusion of water molecules to be restricted [16]. Therefore, the signal in cancerous tissues is higher than normal on DWI. In apparent diffusion coefficient (ADC) maps, which is calculated from DW images, diffusion restriction within the malignant tissue is represented by lower ADC value compared to the normal tissue [17]. However, the benign prostatic hyperplasia (BPH) in transition zones and necrosis of tumor cells also show the same pattern [18]. This could challenge accurate diagnosis of lesions.

The accuracy of qualitative analysis is dependent on the experience of readers and the highest accuracy of prostate cancer detection is 80% in peripheral zone. Quantitative analysis of lesions using radiomics features, as a decision support system, can help radiologists

in more reliable interpretation of images [19]. The aim of this research is to set a method based on quantification of mp-MRI images for discrimination between benign and malignant prostatic lesions with fusion-guided MR imaging/transrectal ultrasonography biopsy as a pathology validation reference.

Material and Methods

It is an analytical research.

Patients

Patients with clinical symptoms, such as higher than normal prostatic specific antigen (PSA) level for three consecutive months, abnormal digital rectal examination (DRE) test and family history of prostate cancer were referred to the MR imaging center by the urologist. Patients who had cardiac pacemakers or other electronic implants, claustrophobia, allergy to gadolinium-based contrast agent and renal insufficiency were not imaged. Other exclusion criteria were history of biopsy, surgery or any therapy for prostate conditions.

A total number of 27 men (mean age 64.2, mean PSA 9.78) were enrolled in this prospective study after obtaining written informed consent between September 2017 and November 2017.

MRI examination

All MRI tests were conducted on a 1.5 Tesla scanner. (Magnetom Avanto, 1.5T, Siemens Healthcare, and Eelangen, Germany) located in Payambaran Hospital, Tehran, Iran. A body coil for signal transmission, a phased-array body coil and an endorectal coil (MEDRAD) for signal readout were used. Mp-MRI sequences were acquired according to minimum standards of prostate imaging report and data system PIRADS (v2) (Figure 1). Detailed imaging protocol can be found in Table 1 [15]. ADC map were generated from MR scanner.

MRI-TRUS biopsy

Each patient with a suspicious area in MR images underwent biopsy. In this method, initially, 3D MRI datasets were imported in the software. The real-time b-mode images of ultrasound examination were then fused with MR images. The MR images were modified and moved in parallel with the ultrasound scan by choosing individual reference points on the MR and b-mode images. This permitted the use of the ultrasound probe, for navigating towards suspicious lesions and performing biopsy.

Based on the 12 core-map of biopsy [20] shown in (Figure 2), one sample was taken from each core and several samples from suspicious areas observed on mp-MRI. The use of mp-MRI improves the accuracy of prostate biopsy. In contrast with traditional biopsy, MRI targeted biopsy has been reported to increase the detection rate of prostate cancer when a similar number of cores are biopsied [21, 22].

Histopathological Assessment

After biopsy, all specimens were sent in formalin container to the pathology ward for histopathology assessment. The pathologist classified each of the specimens in two groups, benign or malignant. The benign group
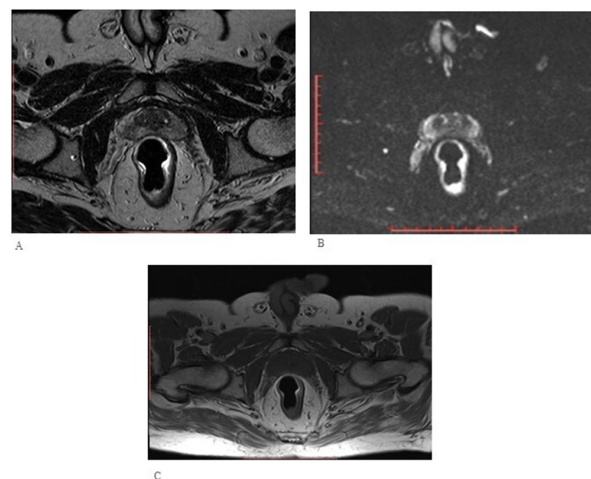

Figure 1: Multiparametric Magnetic Resonance Imaging (MRI) of prostate. A: axial T2 weighted image, B: Diffusion weighted imaging and C: Axial T1 weighted image

Table 1: Multi parametric Magnetic Resonance Imaging (MRI) protocol. The MRI sequences based on the minimum standards of prostate imaging report and data system (PIRADS) (v2).

Sequence	TR (ms)	TE (ms)	FOV (mm)	Slice thickness (mm)	spacing	In plane dimension (phase×frequency) (mm)	b-value
Axial T1w spin echo or gradient echo ± fat sup	506	14	262×300	3	0	≤0.7×≤0.4	-
Multiplannar T2w fast spin echo or turbo spin echo	5650	101	190×190	3	0	≤0.7×≤0.4	-
Axial DW free breathing spin echo EPI seq ±fat sup	3900	99	213×213	3.5	0	≥2.5 for both	50 800 1200

TR: Repetition Time, TE: Echo Time, FOV: Field of View, DW: Diffusion Weighted, EPI: Echo Planar Imaging
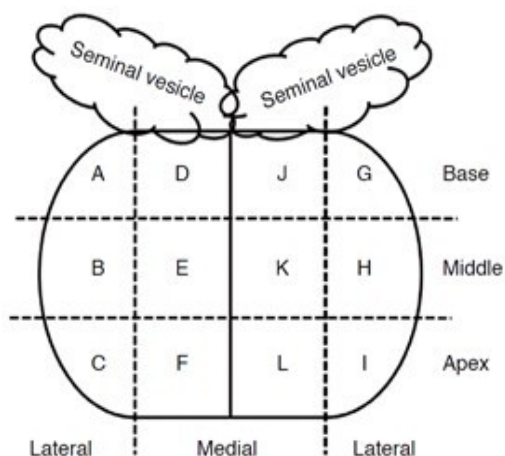
Figure 2: 12-core map for transrectal ultrasound biopsy

included: (1) BPH (benign prostatic hyperplasia), (2) hemorrhage, (3) cysts, (4) calcifications, (5) prostatitis, (6) atrophy, and (7) fibrosis. The malignant group was scored based on the Gleason scoring system. The Gleason score 7(3+4) is an intermediate risk if there is no extraprostatic extension or the volume of tumor is not more than 0.5 cc. The lower than 7(3+4) is low-risk cancer, and

higher than 7(3+4) is high-risk. The results of the 27 specimens are represented in Table 2.

Processing of MR images

Mp-MRI images (Figure 1) were evaluated by a radiologist with more than 15 years of experience in prostate MR imaging. Two-dimensional polygonal regions of interest (ROIs) were placed on all suspicious areas on T2w images (Figure 3), this area was localized based on restriction of diffusion and the contrast enhancement after the injection of gadolinium.

ADC maps were registered to the T2w images as the reference image to transfer the

Table 2: The pathology disturbution Subgroup of pathology and the number of patients in each group

Pathology assessment	Number of patients
Benign	21
Gleason 6	1
Gleason 7 (3+4)	5
Gleason 8	1
Gleason 9	1
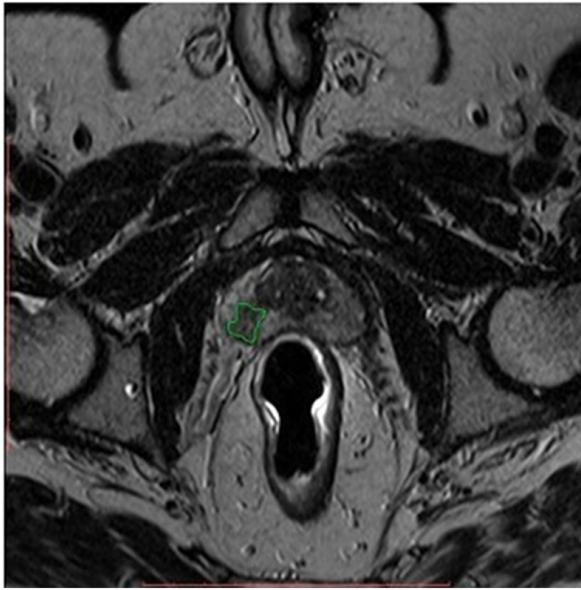
Figure 3: Two-dimensional polygonal regions of interest (ROI) were selected by radiologist on axial T2w image (Green contour).

ROIs to ADC-maps. After registration, the matrix size of ADC-maps became similar to T2 images.

Radiomics Analysis

Four types of regional radiomics features were calculated from the ADC-maps and T2w images to determine the properties of malignant and benign ROIs.

1. First-Order Histogram (FOH) (n=14): FOH analysis is based on image histogram; image histogram is the most straightforward statistical function which measures the number of pixels within the whole ROI with the same signal intensity. Several descriptive features of FOH can describe the properties of benign and malignant tumors.

2. Gray-Level Co-occurrence Matrix (GLCM) (n=23): unlike the global FOH statistics, ignoring the relationship between locally adjacent pixels and the probability of the co-occurrence of the pixel value, GLCM method allows measuring the distribution of pixel pairs, separated by a specific distance and direction. Thus, GLCM captures the fre-

quency of co-occurrence of similar intensity levels over the ROI.

3. Run-Length-Matrix (RLM) (n=44): The run-length matrix reflects the texture's coarseness in a certain direction. A run consists of consecutive pixels in a fixed direction with the same gray-level.

4. Gabor filters (n=25): As a transform-based texture analysis tool, Gabor filters optimally locate image properties in the spatial and frequency domains.

The summary of the features can be found in Table 3.

All these features were computed using in-house software developed using Matlab 2016 b (MathWorks, Natick, MA).

Statistical Analysis

We adopted feature selection with filtering strategy to reduce the dimensionality of the feature space. Receiver-Operating-Characteristic (ROC) analysis was used to estimate the predictive power of radiomics features in predicting the pathological outcome and the area under the curve (AUC) for each feature calculated. The AUC of 0.7 was the thresholds of filtering features. Overall, three feature subsets were created. Subsequently, Linear Discriminant Analysis (LDA) was performed to find the linear combination of features that characterize two pathological classes of parotid tumors (i.e. benign and malignant).

LDA was implemented in leave-one-out cross-validation loops to classify the most frequently selected features in order to prevent overfitting and reducing the potential bias impact of outliers on the diagnostic output of feature selection and classification. In addition, a leave-one-out cross-validation was performed over 27 iterations using the selected feature subset to validate classification output in terms of sensitivity, specificity, and accuracy. By taking averages of these steps over 27 iterations, the result was calculated.

All the analysis was performed using SPSS (v24) and Medcalc.

Results

Table 4 shows the best radiomics-based feature sets constructed for classification of prostate lesions. As it can be observed, subset 1 (T2w) and subset 2 (ADC) resulted in the same accuracy of 88.9%, while the sensitivity and specificity are 95%, 71.4%, respectively for subset 1 and 90.9% and 80% for subset 2. For subset 3 (T2w sand ADC), the accuracy is 92.6% with a sensitivity of 95.2% and speci-ficity of 83.3%. Figure 4 shows the overlap between two pathology subsets when the LDA were performed.

Accuracy, sensitivity and specificity of radiomics-based models for discrimination benign and malignant lesions in prostate (result are shown with 95% confidence interval).

Discussion

In this work, by quantitative analysis, we

Table 3: Summary of radomics faetures used in our work

| Feature classification	Number of features	Features
FOH	14	Mean, Max, Min, Median, Normalized Mean, Standard Deviation (SD), Variance (Smoothness), Energy (Uniformity), Entropy (Irregularity), Third Moment, Kurtosis, 25th, 75th, and 95th Percentile
GLCM	23	Homogeneity Inverse Difference, Inverse Difference Normalized, Inverse Difference Moment Normalized Autocorrelation, Contrast, Correlation1,2, Cluster Prominence, Cluster Shade, Sum Average, Sum Variance, Sum Entropy, Difference Variance, Difference Entropy, Information measure of correlation 1,2, Dissimilarity, Energy, Entropy, Homogeneity1,2, Maximum Probability, Variance,
RLM	44	11 Features in 4 directions (0º,45º,90º,135º): Short-Run Emphasis (SRE)1-4, Long-Run Emphasis (LRE)1-4, Gray-Level Nonuniformity (GLN)1-4, Run-Length Nonuniformity (RLN)1-4, Run Percentage (RP)1-4, Low Gray-Level Run Emphasis (LGRE)1-4, High Gray-Level Run Emphasis (HGRE)1-4, Short-Run Low Gray-Level Emphasis (SRLGE)1-4, Short-Run High Gray-Level Emphasis (SRHGE)1-4, Long-Run Low Gray-Level Emphasis (LRLGE)1-4, Long-Run High Gray-Level Emphasis (LRHGE)1-4
Gabor Texture	25	Rotation-invariant Gabor filters: Gabor1-25

FOH: First-Order Histogram, GLCM: Gray-Level Co-occurrence Matrix, RLM: Run-Length-Matrix
*The values in the parentheses indicate the number of features with different formulations of the same concept.

Table 4: Performances of radiomics-based models

Selected feature subsets	Radiomics-based model	Accuracy (%)	Sensitivity (%)	Specificity (%)
Subset 1(T2w)	SRE-T2w/ Gabor-T2w/ information measure of correlation-T2w/	88.9	95	71.4
Subset 2(ADC)	LRLGE-ADC/ Kurtosis-ADC/GLN-ADC	88.9	90.9	80
Subset 3(ADC and T2w)	SRE-T2w/ Gabor-T2w/ information measure of correlation-T2w/ Gabor-ADC	92.6	95.2	83.3

SRE: Short-Run Emphasis, LRLGE: Long-Run Low Gray-Level Emphasis, ADC: Apparent diffusion coefficient, GLN: Gray-Level Nonuniformity
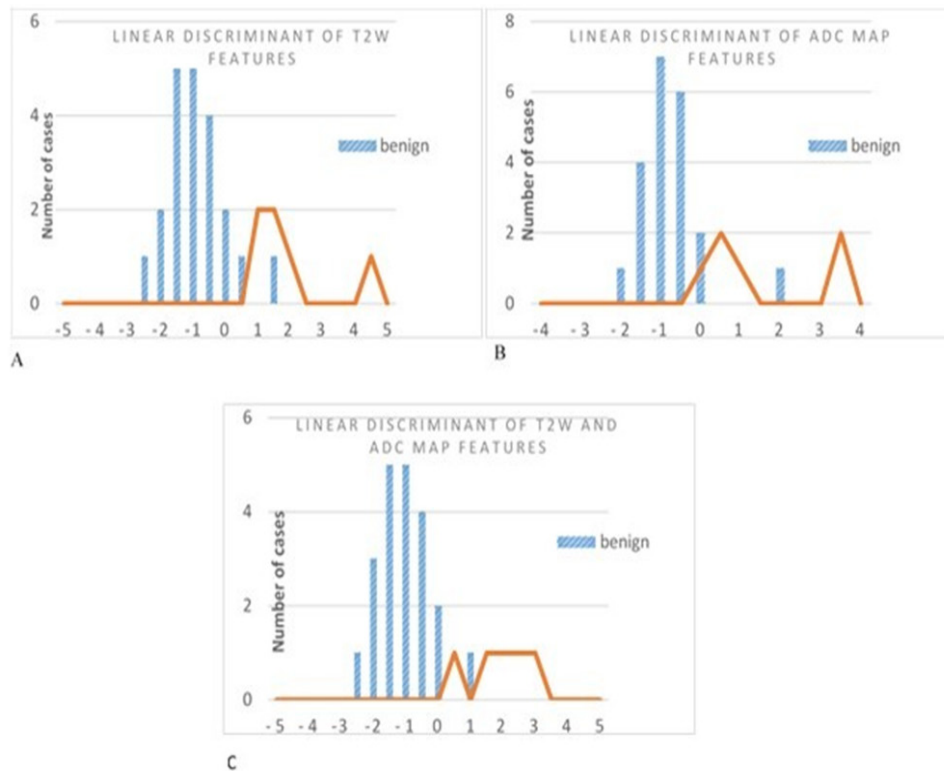
Figure 4: Results of linear discriminant analysis (LDA), each group of features, and the histogram of the two classes of pathology. (ADC: Apparent Diffusion Coefficient)

showed that radiomics-based model extracted from mp-MRI can be predictive of the attributing classes of benign and malignant lesions with 92.6% accuracy which is higher than current diagnostic tools and qualitative analysis of mp-MRI by several studies. It has been shown that qualitative analysis is highly dependent on the experience of readers due to some benign conditions simulating the malignant lesions. The reported accuracy of the qualitative analysis in prostate imaging varies a lot, but the highest accuracy is not higher than 80% so for avoiding over- or underestimating the prostate lesions [23]. We proposed the quantitative analysis of mp-MRI with radiomics feature to provide an accuracy of over 90%. With this promising accuracy, we can avoid biopsies as an invasive method for evaluation of prostate lesions and patients will not suffer from infection, bleeding, pain and other conditions related to biopsy.

In a study performed by Fusco et al. [24] on 21 patients performing mp-MRI (MRSI, DWI and DCE), it was shown that Vp (plasma fraction of Tofts model) median, as a first-order histogram is the best-performing single-parameter (AUC 0.68), while the best parameter combination to discriminate the area with high Gleason score was (Cho+Cr)/Cit (AUC 0.80). Linear discriminant analysis of all features median, including Ktrans, Ve, Vp, D, D*, far zone, Cho+Cr, (Cho+Cr)/Cit and Cit has the accuracy of 71.7% and 80.8% for Gleason score <5 and Gleason score ≥5, respectively. This suggest median as a typical feature-derived does not present high accuracy for differentiating the benign and malignant lesions. In the study of Hoang et al. [25], doing mp-MRI (T2w, DWI, DCE0 on 257 patients), in PZ lesions, eleven quantitative parameters were calculated: normalized T2-weighted signal intensity, T2-weighted signal intensity skewness

and kurtosis, T2 value, wash-in rate, wash-out rate, time to peak (TTP), mean apparent diffusion coefficient (ADC), 10th ADC percentile, and histogram skewness and kurtosis of the ADC value. The best-single parameters in differentiating Gleason score of at least 7 from benign and Gleason score of <7 lesions, were the mean ADC and 10th percentile of ADC with AUC of 0.77 and 0.88, respectively. The best outcomes of combinations of quantitative parameters in the diagnosis of cancers with a Gleason score of at least 7 among PZ lesions at 3 T, using the 10th percentile of ADC as the first variable and the mean ADC as the first variable were the 10th percentile of TTP and the mean ADC and TTP with AUC 0.86 and 0.84 respectively, so that the 10th percentile of ADC with TTP provided accurate results in discriminating cancers with AUC 0.86 and 0.84, respectively. In the study of Hauth et al. [26], mp-MRI (T2w, DWI and DCE) was performed in 110 patients. For malignant and benign lesions, peak-enhancement, initial and post-initial improvement, initial region under the gadolinium curve, Ktrans (forward rate constant), Kep (efflux rate constant), Ve (extracellular volume), ADC (apparent diffusion coefficient) and MR spectroscopy ratio were obtained. Mean, median and the mean to median gap as first-order histogram features were calculated from all parameters and minimum value for ADC (ADC min). The best-performing single-parameters in peripheral zone was ADC min with AUC 0.76 and in transition zone, difference Kep with AUC was 0.75. These studies represent that the first order histogram features are not solely capable to differentiate the benign and malignant lesions with high accuracy.

In some other studies, Khalvati et al. [27], mp-MRI including T2w and DWI performed on 20 patients and two other maps, high-b DWI (CBH-DWI) and correlated diffusion imaging (CDI) were calculated. In this study, besides the first-order histogram features, second-order statistical features (Harlick), Gabor and Kirsch filters were calculated from 8 different imaging modalities (T2w, ADC, CBH-DWI, CDI, b_1(b-value at 0 s/mm^2), b_2(b-value at 100 s/mm^2), b_3(b-value at 400 s/mm^2) and b_4(b-value at 1000 s/mm^2)). All subsets of features from each modality and their combinations were evaluated. The best subset based on the sensitivity and specificity is the one where all modalities are combined together with the accuracy of 82% and 88%, respectively.

In our study, we used four kinds of radiomics features on T2w and ADC map as Table 3. All these features were computed using in-house software developed using Matlab 2016 b (MathWorks, Natick, MA).

This work was designed to find the best model based on radiomics feature to differentiate the benign and malignant cases with an accuracy higher than 90%. The model includes only GLCM, RLM and Gabor features and not the first-order histogram features as first-order histogram features cannot be reliable alone for our goal. The reason for the incapability of histogram features in contrast to GLCM, RLM and Gabor is that histogram features assess the ROI globally and the interrelationships of adjacent voxels in each ROI are ignored.

The limitations that we face in our study were as follows:

1. The small patient population, using a larger dataset, could add more confidence to the radiomics-based models in future work.

2. The small population of the malignant group in our dataset did not allow us to use the proposed model for differentiating lesions with different Gleason scores and evaluating it.

For the future study, considering a big population with a variety of pathology, including different Gleason score lesions, using T2 map instead of T2w images, evaluating dynamic contrast enhancement imaging as another parameter in mp-MRI in 2 different MRI machines in different centers can assess the quantification of mp-MRI based on radiomics feature in all aspects.

Conclusion

In conclusion, radiomics-based methods driven from mp-MRI images could make a potential solution improve the accuracy of diagnosis and differentiate benign and malignant groups in prostate. Therefore, we can avoid biopsies in patients and make a diagnosis based on only mp-MRI and this may allow us to generate the pattern of computer-aided diagnosis system for evaluation of each lesion in the prostate in future.

Authors' Contribution

H. Saligheh Rad and M. Ghafoori conceived of the presented idea. S. Koopaei and M. Alviri developed the theory and performed the computations. A. Fathi Kazerroni and F. Pashaei verified the analytical methods. H. Saligheh Rad encouraged S. Koopaei to investigate [a specific aspect] and supervised the findings of this work. All authors discussed the results and contributed to the final manuscript.

Ethical Approval

The Ethics Committee of Tehran University of Medical Sciences approved the protocol of the study (Ethic cod: IR.TUMS.MEDICINE.REC.1396.3901).

Informed Consent

All patients were informed and consent form were taken for using patient's data in our research.

Funding

This work supported by Tehran University of Medical Science & Health Services [Grant number: 36422, 300496].

Conflict of Interest

None

References

1. Ferlay J, Shin HR, Bray F, Forman D, Mathers C, Parkin DM. Estimates of worldwide burden of cancer in 2008: GLOBOCAN 2008. *Int J Cancer.* 2010;**127**(12):2893-917. doi: 10.1002/ijc.25516. PubMed PMID: 21351269.
2. Verma S, Rajesh A. A clinically relevant approach to imaging prostate cancer. *AJR Am J Roentgenol.* 2011;**196**(3_supplement):S1-10. doi: 10.2214/AJR.09.7196. PubMed PMID: 21343529.
3. Schröder FH. Screening for prostate cancer: current status of ERSPC and screening-related issues. *Recent Results Cancer.* 2014;**202**:47-51. doi: 10.1007/978-3-642-45195-9_5. PubMed PMID: 24531776.
4. Thompson IM, Ankerst DP, Chi C, Lucia MS, et al. Operating characteristics of prostate-specific antigen in men with an initial PSA level of 3.0 ng/ml or lower. *JAMA.* 2005;**294**(1):66-70. doi: 10.1001/jama.294.1.66. PubMed PMID: 15998892.
5. Gretzer MB, Partin AW. PSA markers in prostate cancer detection. *Urologic Clinics of North America.* 2003;**30**(4):677-86. doi: 10.1016/s0094-0143(03)00057-0. PubMed PMID: 14680307.
6. DeSantis C, Ma J, Bryan L, Jemal A. Breast cancer statistics, 2013. *CA Cancer J Clin.* 2014;**64**(1):52-62. doi: 10.3322/caac.21203. PubMed PMID: 24114568.
7. Epstein JI, Feng Z, Trock BJ, Pierorazio PM. Upgrading and downgrading of prostate cancer from biopsy to radical prostatectomy: incidence and predictive factors using the modified Gleason grading system and factoring in tertiary grades. *Eur Urol.* 2012;**61**(5):1019-24. doi: 10.1016/j.eururo.2012.01.050. PubMed PMID: 22336380. PubMed PMCID: PMC4659370.
8. Pokorny MR, De Rooij M, Duncan E, Schröder FH. Prospective study of diagnostic accuracy comparing prostate cancer detection by transrectal ultrasound–guided biopsy versus magnetic resonance (MR) imaging with subsequent MR-guided biopsy in men without previous prostate biopsies. *Eur Urol.* 2014;**66**(1):22-9. doi: 10.1016/j.eururo.2014.03.002. PubMed PMID: 24666839.
9. Phillips R. Stem cells repopulate tumours. *Nat Rev Urol.* 2015;**12**(2):63. doi: 10.1038/nrurol.2014.352. PubMed PMID: 25535001.
10. Bjurlin MA, Carter HB, Schellhammer P, Cookson MS, et al. Optimization of initial prostate biopsy in clinical practice: sampling, labeling and specimen processing. *J Urol.* 2013;**189**(6):2039-46. doi: 10.1016/j.juro.2013.02.072. PubMed PMID: 23485507. PubMed PMCID: PMC3925148.
11. Sanders A, Buchan N. Infection-related hospital admissions after transrectal biopsy of the prostate. *ANZ J Surg.* 2013;**83**(4):246-8. doi: 10.1111/ans.12073. PubMed PMID: 23346881.

12. Utrera NM, Alvarez MB, Polo JM, et al. Infectious complications after transrectal ultrasound-guided prostatic biopsy. Analysis of our experience. *Arch Esp Urol.* 2011;**64**(7):605-10. PubMed PMID: 21965258.

13. Hoeks CM, Barentsz JO, Hambrock T, Yakar D, Somford DM. Prostate cancer: multiparametric MR imaging for detection, localization, and staging. *Radiology.* 2011;**261**(1):46-66. doi: 10.1148/radiol.11091822. PubMed PMID: 21931141.

14. Panebianco V, Barchetti F, Sciarra A, Ciardi A, et al. Multiparametric magnetic resonance imaging vs. standard care in men being evaluated for prostate cancer: a randomized study. *Urol Oncol.* 2015;**33**(1):e1-17. doi: 10.1016/j.urolonc.2014.09.013. PubMed PMID: 25443268.

15. Weinreb JC, Barentsz JO, Choyke PL, et al. PI-RADS prostate imaging–reporting and data system: 2015, version 2. *Eur Urol.* 2016;**69**(1):16-40. doi: 10.1016/j.eururo.2015.08.052. PubMed PMID: 26427566. PubMed PMCID: PMC6467207.

16. Desouza NM, Reinsberg SA, Scurr ED, Brewster JM, Payne GS. Magnetic resonance imaging in prostate cancer: the value of apparent diffusion coefficients for identifying malignant nodules. *Br J Radiol.* 2007;**80**(950):90-5. doi: 10.1259/bjr/24232319. PubMed PMID: 17303616.

17. Elbuluk O, Turkbey B, Choyke P. Prostate Imaging, InInterventional Urology. Springer International Publishin; 2016. p. 59-72.

18. Haider MA, Van Der Kwast TH, Tanguay J, et al. Combined T2-weighted and diffusion-weighted MRI for localization of prostate cancer. *AJR Am J Roentgenol.* 2007;**189**(2):323-8. doi: 10.2214/AJR.07.2211. PubMed PMID: 17646457.

19. Fathi Kazerooni A, Nabil M, Haghighat Khah H, Alviri M, et al ADC-derived spatial features can accurately classify adnexal lesions. *J Magn Reson Imaging.* 2018;**47**(4):1061-71. doi: 10.1002/jmri.25854. PubMed PMID: 28901638.

20. You MW, Kim MH, Kim JK, Cho KS. The characteristics and spatial distributions of initially missed and rebiopsy-detected prostate cancers. *Ultrasonography.* 2016;**35**(3):226. doi: 10.14366/usg.15065. PubMed PMID: 27048261. PubMed PMCID: PMC4939716.

21. Abdi H, Zargar H, Goldenberg SL, Walshe T, et al. Multiparametric magnetic resonance imaging–targeted biopsy for the detection of prostate cancer in patients with prior negative biopsy results. *Urol Oncol.* 2015;**33**(4):165.e1-7. doi: 10.1016/j.urolonc.2015.01.004. PubMed PMID: 25665509.

22. Javali TD, Dwivedi DK, Kumar R, Jagannathan NR, et al. Magnetic resonance spectroscopy imaging-directed transrectal ultrasound biopsy increases prostate cancer detection in men with prostate-specific antigen between 4-10 ng/mL and normal digital rectal examination. *Int J Urol.* 2014;**21**(3):257-62. doi: 10.1111/iju.12258. PubMed PMID: 23980749.

23. Bae H, Yoshida S, Matsuoka Y, Nakajima H, et al. Apparent diffusion coefficient value as a biomarker reflecting morphological and biological features of prostate cancer. *Int Urol Nephrol.* 2014;**46**(3):555-61. doi: 10.1007/s11255-013-0557-1. PubMed PMID: 24022845.

24. Fusco R, Sansone M, Petrillo M, Setola SV, et al. Multiparametric MRI for prostate cancer detection: Preliminary results on quantitative analysis of dynamic contrast enhanced imaging, diffusion-weighted imaging and spectroscopy imaging. *Magnetic Resonance Imaging.* 2016;**34**(7):839-45. doi: 10.1016/j.mri.2016.04.001. PubMed PMID: 27071309.

25. Hoang Dinh A, Melodelima C, Souchon R, et al. Quantitative analysis of prostate multiparametric MR images for detection of aggressive prostate cancer in the peripheral zone: a multiple imager study. *Radiology.* 2016;**280**(1):117-27. doi: 10.1148/radiol.2016151406. PubMed PMID: 26859255.

26. Hauth E, Halbritter D, Jaeger H, Hohmuth H, Beer M. Diagnostic value of semi-quantitative and quantitative analysis of functional parameters in multiparametric MRI of the prostate. *TBr J Radiol.* 2017;**90**(1078):20170067. doi: 10.1259/bjr.20170067. PubMed PMID: 28749167.

27. Khalvati F, Wong A, Haider MA. Automated prostate cancer detection via comprehensive multiparametric magnetic resonance imaging texture feature models. *BMC Med Imaging.* 2015;**15**(1):27. doi: 10.1186/s12880-015-0069-9. PubMed PMID: 26242589. PubMed PMCID: PMC4524105.